Simulation of one-dimensional elastic wave generated by plate impact

Abstract. This report presents a working simulation of elastic shock wave from a symmetric plate impact, i.e. an impact where the material for the impactor and the target are same. The simulation is restrict to elastic deformation regime and plane strain scenario, these simplifications make sure that the simulation is within the scope of the course while maintaining a certain level of challenge. In the simulation, an artificial viscosity term is included in order to capture the rapid change of state variables such as particle velocity, pressure and density, etc, at the vicinity of the shock front. Stability requirements are also calculated to make sure the simulation result is valid.

Introduction. The shocks manifest themselves mathematically as surfaces on which density, velocity, temperature, and entropy, etc, have discontinuities, and the partial differential equations governing the motion of require boundary conditions connection the values of these quantities on the two sides of each such surface, i.e. the shock front. The necessary boundary conditions are known as the Rankine-Hugoniot equations. However, the application of them in a numerical simulation is complicated as the shock front is in motion relative to the space-time frame, and the motion is not known in advance but is governed by the

differential equations and boundary conditions themselves.

In this circumstance, simulations without above mentioned boundary conditions are carried out. This method is employed by introducing an artificial dissipative terms, such as viscosity and heat conduction. When viscosity, for example, is taken into account, the shocks are seen to be smeared out, so the discontinuities are replaced by rapid changes within a very thin layer. The thickness of the layer is designed to be of the same order of the mesh width, and the dissipative term goes to zero at any points far away from the layer. This guarantees the physical authenticity of the shock, where dissipative reactions happen only at the neighboring of the shock front.

Method. The simulation presented in the report uses central difference method. Staggered mesh are used in the simulation, the particle velocities are stored in nodes centered in space and at half steps in time, whereas all the other variables are stored in nodes centered in time and at half steps in time. Aluminum is used in this project. The deformation in the area swiped by the shock front can be treated as one-dimensional, as the displacement perpendicular to the shock propagating direction (transverse deformation) is zero due to the symmetry of the geometry. Furthermore, the deformation behind the shock front are assumed to be within elastic regime, thus the deformation and the stress can be related by Hook's law.

The governing equation are expressed as follows:

$$\rho_0 \frac{\partial v_i}{\partial t} = \frac{\partial P_{i1}}{\partial X_1} - \frac{\partial q}{\partial X_1} \delta_{i1} \tag{1}$$

$$\frac{\partial F_{i1}}{\partial t} = \frac{\partial v_i}{\partial X_1} \tag{2}$$

where,

v_i is the i-th component of particle velocity vector.

P_{i1} is the i-th row, first column component of the first Piola-Kirchhoff stress tensor.

F_{i1} is the i-th row, first column component of the deformation gradient tensor.

q is the artificial dissipative term.

δ_{i1} is Kronecker delta.

For one-dimensional deformation where the deformation is along X_1 direction, the deformation gradient tensor is expressed as:

$$\boldsymbol{F} = \begin{bmatrix} F_{11} & 0 & 0 \\ 0 & 1 & 0 \\ 0 & 0 & 1 \end{bmatrix}$$

The Lagrangian strain tensor is then:

$$\boldsymbol{E} = \frac{\mathbf{1}}{\mathbf{2}}(\boldsymbol{F}^T\boldsymbol{F} - \boldsymbol{I}) = \frac{1}{2}\begin{bmatrix} F_{11}^2 - 1 & 0 & 0 \\ 0 & 0 & 0 \\ 0 & 0 & 0 \end{bmatrix}$$

For deformation within linear elastic limit, the second Piola-Kirchhoff stress tensor is:

$$S_{ij} = \frac{E}{1+\nu} E_{ij} + \frac{E\nu}{(1+\nu)(1-2\nu)} E_{kk}\delta_{ij} \tag{3}$$

where

S_{ij} is the i-th row, first column component of the second Piola-Kirchhoff stress tensor.

E_{ij} is the i-th row, first column component of the Lagrangian strain tensor.

E, ν are Young's modulus and Poisson's ratio, respectively.

For the case of one-dimensional strain, since the only non-zero term of $\boldsymbol{E}$ is E_{11}, thus (3) can be expressed in terms of a scalar equation:

$$S_{11} = CE_{11} \tag{4}$$

where $C = \frac{E}{1+\nu} + \frac{E\nu}{(1+\nu)(1-2\nu)}$. S_{21} and S_{31} are both zero.

The first Piola-Kirchhoff stress tensor $\boldsymbol{P}$ is expressed as

$$\boldsymbol{P} = \boldsymbol{FS}$$

From (4), we have

$$P_{11} = F_{11}S_{11} = \frac{C}{2}(F_{11}^3 - F_{11}) \tag{5}$$

P_{21} and P_{31} are both zero.

With (5), (1) and (2) can be written in discretized form as

$$\rho_0 \frac{v_m^{n+\frac{1}{2}} - v_m^{n-\frac{1}{2}}}{\Delta t} = \frac{P^n_{m+\frac{1}{2}} - P^n_{m-\frac{1}{2}}}{\Delta X} - \frac{q^n_{m+\frac{1}{2}} - q^n_{m-\frac{1}{2}}}{\Delta X} \tag{6}$$

$$\frac{F^{n+1}_{m+\frac{1}{2}} - F^n_{m+\frac{1}{2}}}{\Delta t} = \frac{v_{m+1}^{n+\frac{1}{2}} - v_m^{n+\frac{1}{2}}}{\Delta X} \tag{7}$$

The dissipative term q has the form

$$q^n_{m+\frac{1}{2}} = \rho_0 \left(C_L a_1 \left| \Delta v^{n-\frac{1}{2}}_{m+\frac{1}{2}} \right| + a_2 \left(\Delta v^{n-\frac{1}{2}}_{m+\frac{1}{2}} \right)^2 \right) \tag{8}$$

where $\Delta v_{m+\frac{1}{2}}^{n-\frac{1}{2}} = v_{m+1}^{n-\frac{1}{2}} - v_m^{n-\frac{1}{2}}$. C_L is longitudinal sound speed in the material, a_1 and a_2 are constants to be determined.

From (8), it can be seen that q is non-zero only at the neighbor of the shock front as otherwise $v_{m+1}^{n-\frac{1}{2}} = v_m^{n-\frac{1}{2}}$. In (6)~(8), all indices refer to tensor components are dropped because both side of above equations equal to zero unless $i = 1$. Equation (6)~(8) provide a complete circle for calculating particle velocity v, deformation gradient tensor $\boldsymbol{F}$ (hereafter scalar F), and first Piola-Kirchhoff stress tensor $\boldsymbol{P}$ (hereafter scalar P).

To investigate the stability condition as well as the stability of the differential equation, we need to see what the solution behaves when we impose a small perturbation on the solution. Suppose we have the solution for F, P, v, q, we now replace those terms by $\delta F, \delta P, \delta v, \delta q$. The dissipative term can be expressed in differential form:

$$q_{m+\frac{1}{2}}^{n} = \rho_0 \left(C_L a_1 \left| v_{m+1}^{n-\frac{1}{2}} - v_m^{n-\frac{1}{2}} \right| + a_2 \left(v_{m+1}^{n-\frac{1}{2}} - v_m^{n-\frac{1}{2}} \right)^2 \right)$$

$$= \rho_0 \left(C_L a_1 \Delta X \left| \frac{v_{m+1}^{n-\frac{1}{2}} - v_m^{n-\frac{1}{2}}}{\Delta X} \right| + a_2 (\Delta X)^2 \left(\frac{v_{m+1}^{n-\frac{1}{2}} - v_m^{n-\frac{1}{2}}}{\Delta X} \right)^2 \right)$$

$$q = \rho_0 \left(C_L a_1 \Delta X \left| \frac{\partial v}{\partial X} \right| + a_2 (\Delta X)^2 \left(\frac{\partial v}{\partial X} \right)^2 \right) \qquad (9)$$

Equation (1), (2), (5), after expressing every variable in terms of scalars, now become:

$$\rho_0 \frac{\partial v}{\partial t} = \frac{\partial P}{\partial X_1} - \frac{\partial q}{\partial X_1} \qquad (10)$$

$$\frac{\partial F}{\partial t} = \frac{\partial v}{\partial X_1} \tag{11}$$

$$P = \frac{C}{2}(F^3 - F) \tag{12}$$

Write (9)~(12) in terms of first variation:

$$\rho_0 \frac{\partial \delta v}{\partial t} = \frac{\partial \delta P}{\partial X_1} - \frac{\partial \delta q}{\partial X_1} \tag{13}$$

$$\frac{\partial \delta F}{\partial t} = \frac{\partial \delta v}{\partial X_1} \tag{14}$$

$$\delta P = \frac{C}{2}(3F^2 \delta F - \delta F) \tag{15}$$

$$\delta q = A\left|\frac{\partial \delta v}{\partial X}\right| + 2B\frac{\partial v}{\partial X}\frac{\partial \delta v}{\partial X} \tag{16}$$

where $A = \rho_0 C_L a_1 \Delta X$ and $B = \rho_0 a_2 (\Delta X)^2$

We look for the solution that has the form:

$$\delta U = \delta U_0 e^{ikx+\alpha t} \tag{17}$$

where U represent variables v, P, F, q. Substitute (17) into (13)~(16), then we have four linear equations in terms of $\delta v_0, \delta P_0, \delta F_0, \delta q_0$. The system of equations is solved by equating the determinant of the coefficients matrix to zero. The determinantal equation is:

$$-\rho_0 \alpha + Ak^2 + 2B\frac{\partial v}{\partial X}k^2 + \left(Ak^2 + 2B\frac{\partial v}{\partial X}k^2\right)\left(\frac{1}{2}C - \frac{3}{2}CF^2\right) = 0 \tag{18}$$

From (18), we can get an expression for α:

$$\alpha = -\frac{k^2}{\rho_0}\left(A + 2B\frac{\partial v}{\partial X}\right)\left[\frac{C}{2}(3F^2 - 1) - 1\right] \qquad (19)$$

In a deformation, the volume change is expressed in terms of the Jacobian J, which is the determinant of deformation gradient tensor $\boldsymbol{F}$. Suppose the density in the original and deformed configuration are ρ_0 and ρ, respectively, then from the conservation of mass, $\rho_0 = \rho J$. From earlier discussion, $\boldsymbol{F}$ is diagonal matrix where $F_{22} = F_{33} = 1$, and $F_{11} = F$, thus $\rho_0 = \rho F$. For a moderate plate impact where density barely changes, F is of order of 1 (~0.97). Thus the terms in the bracket on the right hand side of (19) is positive. To make sure the perturbation doesn't grow, we need to make sure that α is non-positive, this is achieved by choosing a_1, a_2 such that $\left(A + 2B\frac{\partial v}{\partial X}\right)$ is positive.

The above discussion is limited in shock region, where the dissipative term is taken into account. Similar investigation can be performed in the normal region by considering (13)~(15), but drop any terms containing q. Repeat the previous procedure, we get for normal region:

$$\alpha^2 = -\frac{k^2 C}{2\rho_0}(3F^2 - 1) \qquad (20)$$

From (19) and (20), we have seen that the differential equation is stable, i.e. the error either damps out or doesn't grow.

We can furthermore rewrite (19) and (20):

$$\frac{\partial \delta v}{\partial t} = \sigma \frac{\partial^2 \delta v}{\partial x^2} \qquad (21)$$

$$\frac{\partial^2 \delta v}{\partial t^2} = s^2 \frac{\partial^2 \delta v}{\partial x^2} \tag{22}$$

where $\sigma = C_L a_1 \Delta X + 2a_2 (\Delta X)^2 \frac{\partial v}{\partial X} \left[\frac{C}{2}(3F^2 - 1) - 1\right]$

$s^2 = \frac{C}{2\rho}(3F^2 - 1)$.

The von-Neumann stability inequalities for (21) and (22) are

$$\Delta t \leq \frac{1}{2}\frac{\Delta X}{\sigma}$$

And

$$\Delta t \leq \frac{\Delta X}{s}$$

Results. The domain is from 0 to 2 mm, in which the impactor is from 0 to 1.1 mm and the target is from 1.1 mm to 2 mm. The total duration is 3 μm. Impact velocity is 300 m/s. Mesh width and time step are 2 μm and 10 ps, respectively. a_1 and a_2 are 0.06 and 2, respectively. The time-space frame is illustrated in Figure 1. Figure 2 is the simulated result.

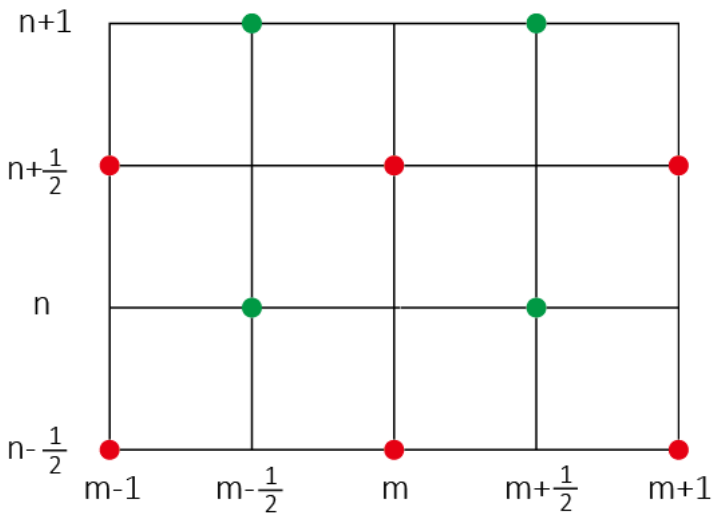

Figure 1. Illustration of time-space frame. v is stored in red nodes, and P, F, q are stored in green nodes.

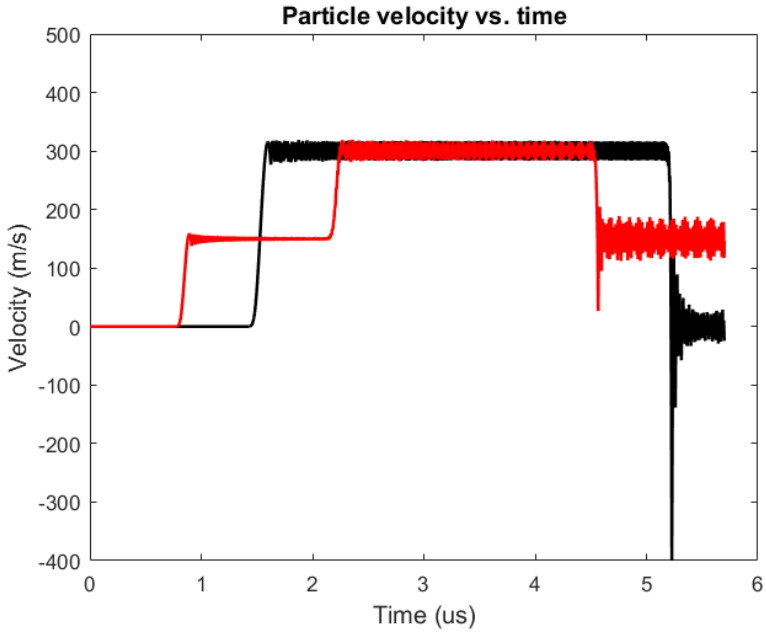

Figure 2. Particle velocity at two locations. The red line represents the point in the center of the target, whereas the black line represents the point at the free surface of the target.

The simulation agrees with the analytical solution. In a symmetric plate impact, the states behind the shock front can be calculated using Rankine-Hugoniot jump condition. The shock speed in an aluminum-aluminum plate impact with impact velocity equal to 300 m/s is 5.6 km/s. For particles at the free surface (L=0.9 mm) and at the center (L=0.45 mm), the first discontinuity occurs at 1.6 μs and 0.8 μs, respectively. We can also calculate the particle velocities at those two locations. From the jump condition, in a symmetric impact, for any interior location, the particle velocity is half of the impact speed after swiped by the first shock wave, and the area is in compression. At free surface, with the absence of pressure, the particle velocity is doubled, hence equal to the impact speed. This is true for any location without pressure. When the wave hits the free

surface and bounces back, it forms a travelling tension wave that travels at opposite direction. This tension wave cancels out the compression in the interior and brings the particle velocity to the same level of that for free surface. Since the tension wave travels at a same speed as the compression wave, we would expect a second discontinuity in the red line that happens at approximately 2.4 μs.

To better see the role of dissipative term, we also performed simulation without it. The results is shown in Figure 3.

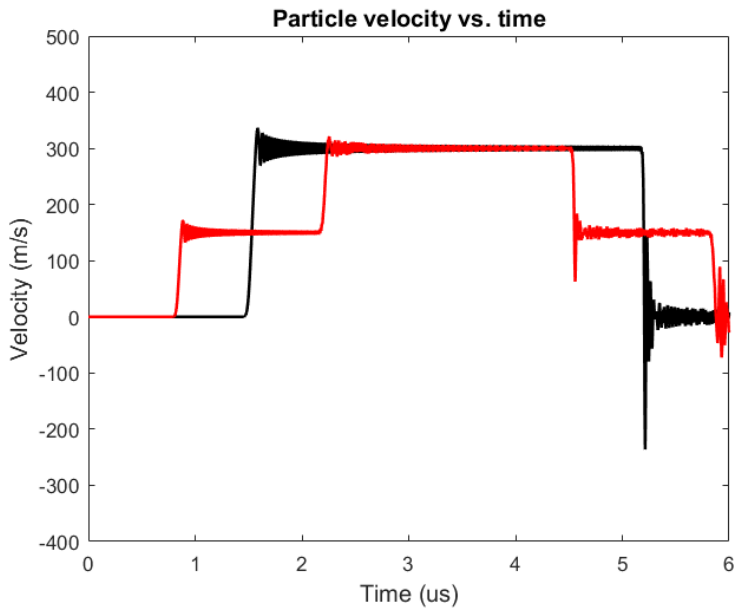

Figure 3. Particle velocity profile without artificial dissipative term

Surprisingly, the result doesn't blow up as we expected. Moreover, it is even better than the previous results in some region. Compare the part where velocity is 300 m/s, the result shown in Figure 2 obviously has more oscillation than that shown in Figure 3. However, for the interior part swiped by the compression wave (first jump in the red lines), the result in

Figure 2 converges faster than that in Figure 3. Two possible reasons that may cause this, one is because of the pattern of reflected wave, the other one is the state of stress in the region.

The wave reflected from an interface tends to spread out if the material at the other side of the interface has smaller impedance. In this case, multiply waves with less strength reflect back from the free surface, as it is are that is at the other side, which has smaller impedance.

To investigate what is the reason, two more simulations are performed. The first one is to attach another layer of material with higher impedance, such as copper, to the free surface of the target. The second one is to drop dissipative term when the material is in tension. The state of stress is determined by the rate of the strain, where a positive rate indicates the material is in tension, and a negative rate indicates the material is in compression. The results for above simulations are shown in Figure 4 and Figure 5.

Figure 4 shows the interior particle velocity when a layer of copper is attached to the free surface of the target. Since copper has larger impedance than aluminum, the reflected wave stays in one piece. However, same pattern of oscillation is still observed. On the other hand, in Figure 5, the result where dissipative term is dropped behaves almost exactly the same as the analytical solution. Here we say ‘almost’ because there is a finite rising time in the plot, where for the case of analytical

solution it would have been a clean jump.

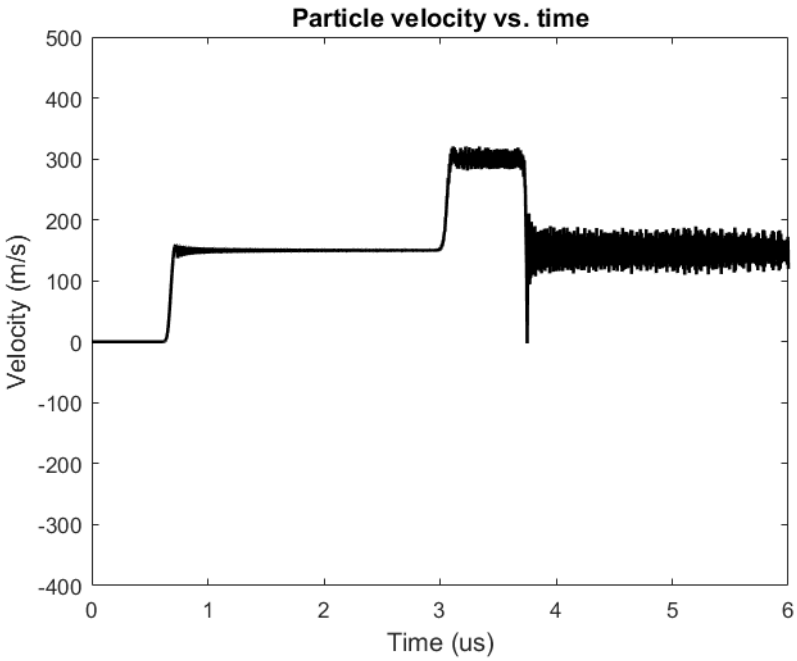

Figure 4. Interior particle velocity. Free surface is attached to copper.

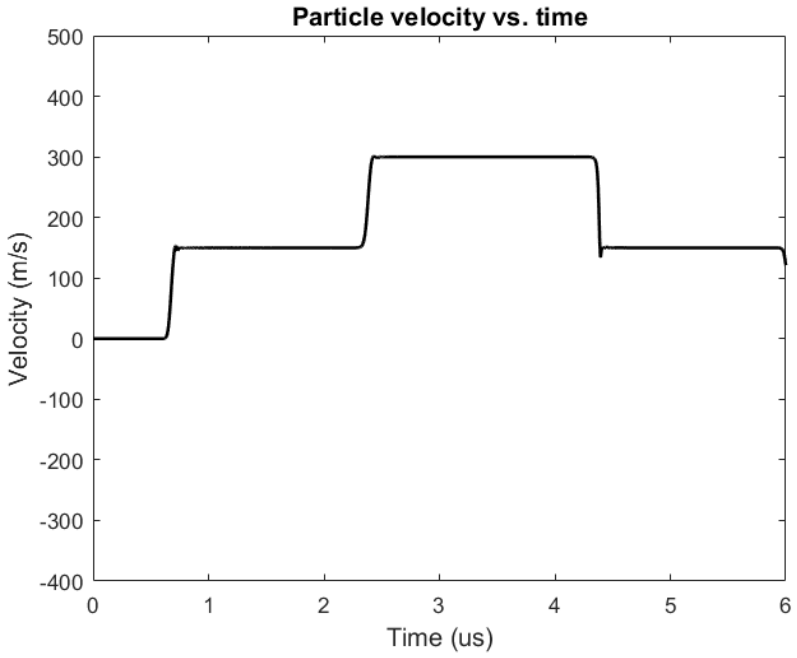

Figure 4. Interior particle velocity. Dissipative term is dropped if in tension.

Conclusion. The above discussed results demonstrate the role of the artificial dissipative term introduced in plate impact simulation. Even though the study is restricted to the simplest case, where the deformation is taken as one-dimensional and elastic, we can still see that by introducing dissipative term, the quality of simulation results improves. The improvement is believed to be even more significant when we are to deal with pressure shear plate impact, where we also have transverse particle velocity, and in the regime of thermoelastic-viscoplastic. In the latter case, the results will blow up without the dissipative term.

References

[1] VonNeumann, J., & Richtmyer, R. D. (1950). A Method for the Numerical Calculation of Hydrodynamic Shocks. Journal of Applied Physics, 21(3), 232–237. https://doi.org/10.1063/1.1699639

[2] Lloyd, J. T., & McDowell, D. L. (2014). Microstructure-sensitive simulation of shock loading in metals (dissertation). Georgia Institute of Technology, Atlanta, GA.

[3] Courant, R., Friedrichs, K., & Lewy, H. (1986). On the Partial Difference Equations of Mathematical Physics. Kurt Otto Friedrichs, 96–115. https://doi.org/10.1007/978-1-4612-5385-3_8

[4] Reddy, J. N. (2013). An introduction to continuum mechanics. Cambridge University Press.

[5] Saada, A. S. (2009). Elasticity: theory and applications. J Ross Pub.